Supporting Information

Kursar et al. 10.1073/pnas.0904786106

SI Text

Sample Collection. Ecological data were taken for young leaves on saplings (0.5–2.5 m tall) growing in the understory. More than 50 km of trails were walked regularly to search for plants with young leaves. Panamanian collections were made from March 2001 to November 2004, and Peruvian collections were made from May to December 2007.

Rates of leaf expansion were determined by measuring the area of marked leaves every 1–3 days throughout expansion. Expansion rates were calculated as the percentage increase in area per day for leaves between 20% and 80% of full size. Because of herbivore damage, many leaves had to be excluded so expansion data were based on an average of 13 individual leaves per species. Because temperatures differed by 3.9 °C between the study sites/seasons, we adjusted expansion rates from Peru by a factor of 1.51, equivalent to a Q_{10} of 2.7 that we have measured for respiration in tropical leaves. The number of ants visiting extrafloral nectaries of young leaves was counted (# nectary^{-1}) during censuses along trails between 10 AM and 3 PM for an average of 83 plants per species. Chlorophyll content (mg·m^{-2}) was determined for an average of nine young leaves per species estimated to be between 60% and 80% of full size. A known area of leaf tissue was homogenized in 95% ethanol and centrifuged, and absorbances at 663 and 725 nm were measured with a portable spectrophotometer (Milton Roy, Spectronic Mini 20). See Table S3 for values and sample sizes averaged by species.

Chemical Analyses. Young leaves were collected from understory saplings and were between 10% and 90% of full expansion. Less than 1/3 of the leaves on a single flush were collected to minimize negative impacts to the plant. For each species, leaves were collected from many different plants and stored separately. Most of the leaves collected in Panama were homogenized in 95% ethanol by using a Polytron (Brinkmann Instruments) and then stored at −50 °C until shipped to Utah for analysis. Some samples from Panama and all leaves collected in Peru were dried under vacuum (<1 Torr in Panama or 10 Torr, with silica gel, in Peru) for 36–48 h and then stored at −50 °C in Panama and −15 °C in Peru in doubly sealed plastic bags with silica gel until being shipped to Utah. Extracts of young leaves from 37 *Inga* species from Panama and Peru were analyzed for phenolic and saponin content. Panamanian samples were also analyzed for nonprotein amino acids.

Phylogenetic Reconstruction. PCR and sequencing protocols for trnD-T are given in ref. 1. The psbA-trnH region was amplified and sequenced with primers psbA GTTATGCATGAACGTAATGCTC and trnH CGCGCATGGTGGATTCAAATCC. The rps16 regions was amplified and sequenced with primers rps16-F GTGGTAGAAAGCAACGTGCGA and rps16-R TCGGGATCGAACATCAATTGCAAC. PCR conditions for psbA-trnH and rps16 were: one cycle of 94 °C for 2 min; 30 cycles of 94 °C for 1 min, 50 °C for 1 min, and 72 °C for 1 min; one cycle of 72 °C for 10 min. The trnL-F region was amplified and sequenced in two parts by using primer pairs trnL c CGAAATCGGTAGACGCTACG, trnL d GGGGATAGAGGGACTTGAAC, and trnL e GGTTCAAGTCCCTCTATCCC, trnL f ATTTGAACTGGTGACACGAG. PCR conditions for trnL-F were: one cycle of 94 °C for 4 min; 35 cycles of 94 °C for 45 s, 55 °C for 45 s, and 72 °C for 3 min; one cycle of 72 °C for 10 min. The ndhF-rpl32 region was amplified and sequenced following Shaw et al. (2), and rpoC1 was amplified and sequenced following Hollingsworth et al. (3). For the ≈50% of samples that did not produce PCR products for ndhF-rpl32 using Shaw et al. (2) protocols, we developed new primers (forward: GGAGCTGCCATTCCAAAAT; reverse: TTCGCCAATTTTATCTCTTTTG) and new PCR conditions: one cycle of 94 °C for 2 min; 30 cycles of 95 °C for 1 min, 48 °C for 1 min, 65 °C for 4 min with ramp of 0.3/s to 65 °C; one cycle of 65 °C for 5 min. For psbA-trnH, rps16, rpoCI, ndhF-rpl32 and trnL-F, the 25-μL reaction mix consisted of 16.1 μL of H_2O, 2.5 μL of *Taq* buffer, 2.5 μL of dNTP mix (10 mM concentration for each nucleotide), 0.75 μL of each primer (10 μM concentration), 1.25 μL of $MgCl_2$ (50 mM concentration), 0.125 μL of *Taq* polymerase (0.625 units), and 1 μL of DNA template. In some cases of nonamplification, 2 μL of DNA template was used (with the volume of H_2O adjusted accordingly. Cleaned PCR products were sequenced by using ABI capillary sequencers (Applied Biosystems) at the University of Edinburgh and Northwoods DNA. Sequences were assembled by using Sequencher v4.5 (Gene Codes) and aligned manually, which was unproblematic given low sequence divergence.

Bayesian analysis was performed by using MrBayes 3.1.1 (4) with 5,000,000 generations of four simultaneous MCMC chains, sampling one tree every 10,000 generations. ModelTest 3.7 (5) was used to select the best-fitting substitution model for each plastid region. Phylogenetic trees were rooted by using outgroup sequences from *Zygia*, which is shown to be most closely related to *Inga* in phylogenetic analyses by using multiple genera from tribe Ingeae.

We ran initial analyses using all accessions from both Peru and Panama. Because in all cases accessions of species found in both Peru and Panama were resolved as monophyletic, or nearly so, we reduced each to a single accession so as not to bias analyses attempting to detect phylogenetic signal.

For subsequent ecological analyses that involved phylogenies, we randomly selected 100 or 200 after burn-in phylogenetic trees from the Bayesian phylogenetic analysis. All trees were made ultrametric before subsequent analyses by using nonparametric rate smoothing (6) in the APE package (7) of the R statistical environment (R Core Development Team 2009). All analyses were also conducted by using a set of 173 equally parsimonious trees and gave equivalent results.

Relationships Among Defense Traits. We evaluated relationships between expansion rate, chlorophyll content, and ant visitation for all species by using conventional least-squares linear regression and linear models with PICs and forcing the intercept through zero (8). For analyses that involved all species, trait values were averaged between Peru and Panama for shared species. Analyses were conducted in the R statistical environment (R Core Development Team 2009). We report r^2 values adjusted for sample size and parameter number. PICs were obtained by using the APE package in R. For the ant visitation character, differences among species in visitation rates were compared by using data that were normalized for each site because ant abundance was >2 times higher in Peru.

Chemical Defense Similarity. We evaluated chemical dissimilarity (or distance) between species as the total number of compounds for which they differed in presence/absence state, standardized by the maximum value for this metric across all species pairs (thus, distance varies from 0 to 1). We first calculated dissimilarity separately for phenolics and saponins. To obtain the total

chemical distance between species, we combined the phenolics and saponins data and upweighted saponins such that the maximum distance for saponins would be equal to the maximum distance for phenolics. For BCI Inga, we also calculated the chemical distance for nonprotein amino acid composition. We evaluated the correlation between chemical distances and phylogenetic distance (across the 200 Bayesian trees) by using Mantel tests (9).

We constructed a dendrogram for the chemical composition data by using hierarchical clustering (10) of the equally weighted phenolics and saponins data. We assessed support for the dendrogram by using multiscale bootstrapping and calculating the approximately unbiased P values for nodes with the pvclust package (11) in R.

Evolutionary Lability in Escape vs. Defense and Ant Visitation. Because the above analyses indicated that expansion rate and chlorophyll content covaried strongly, we used a PCA to derive independent axes of defense trait variation for variables for which we had continuous data (expansion rate, chlorophyll content, and ant visitation). The PCA produced two axes with eigenvalues >1. The first axis was highly correlated with expansion rate ($r = -0.71$) and chlorophyll content ($r = 0.70$), whereas the second axis was highly correlated with ant visitation ($r = 0.98$).

We assessed whether there was significant phylogenetic signal for these two defense axes by determining whether Blomberg's K (12) was significantly different from 0, based on 999 randomizations of the data (across 200 Bayesian trees; using the R package Picante; http://picante.r-forge.r-project.org).

We were lacking expansion rate or chlorophyll content data for 1/3 of the species in Peru. To include these species in analyses, we derived a binary characterization, which represented the two extremes of the developmental defense syndrome. For species with chlorophyll and expansion data, species were classified as escape vs. defense (13) based on where the species were placed on a plot of expansion rate by chlorophyll content (see Fig. 2). For most of the remaining species where data were incomplete, T.A.K. and P.D.C. classified them as escape or defense by using their extensive field experience with visually estimating chlorophyll content (Table S3).

We assessed phylogenetic signal for this escape/defense character by optimizing the character under a maximum parsimony criterion onto the 50% majority rule Bayesian consensus tree by using Mesquite version 2.01 (Fig. S4 and ref. 14). To account for topological uncertainty, the procedure "Trace over Trees" was used to summarize ancestral state reconstructions >100 Bayesian trees sampled at stationarity. To test whether phylogenetic distribution of escape/defense was significantly different from random the number of parsimony steps in these characters was measured across 100 Bayesian trees sampled at stationarity was compared with: (*i*) the number of steps in the same characters optimized on to 1,000 random trees produced in MacClade 4.08 (15) and (*ii*) the number of steps in the same characters when the states were randomized among terminal taxa using the "reshuffle character" option in Mesquite (14). We used a similar approach to visualize the evolution of a binary character representing ant visitation rates (high vs. low visitation; Fig. S4).

We also determined whether developmental and ant defense axes (axes 1 and 2, respectively, from PCA analyses above) were orthogonal to chemical defenses. We first obtained distance matrices for these axes by calculating the Euclidean distance between species for each axis. We then used Mantel tests to assess whether there was a significant correlation between each distance matrix and the chemical distance matrix.

Community Phylogenetic and Defense Trait Dispersion. We evaluated the phylogenetic and defense trait structure of Inga communities by using the inverse of the NRI and NTI of Webb (16) and as calculated following Kembel and Hubbell (17). We conducted analyses separately for Panama and Peru and only used species from each location when randomly drawing species for null communities. We shuffled tip labels in the phylogeny (18) to generate null communities for calculating the normalized metrics NRI and NTI. There was no significant phylogenetic signal for abundance in Peru or Panama (across 200 Bayesian trees; Peru: $\bar{K} = 0.64$, $\bar{P} = 0.36$; Panama: $\bar{K} = 0.96$, $\bar{P} = 0.12$), although lack of significance may be caused by low sample size, particularly in Panama.

We calculated a defense distance matrix between species separately for Peru and Panama by averaging the distance matrices for the different chemical classes above (the nonprotein amino acid matrix being present for Panama only) with an ant visitation rate distance matrix (absolute distance between species in ant visitation rate, standardized by the maximum value) and an escape vs. defense distance matrix (where matrix cells have a binary state of 1 if the two species differ in this classification and 0 if they are the same). Thus, the different chemical defense classes, ant visitation rate, and escape vs. defense were all weighted equally. We obtained a bio-neighbor joining tree from the total defense distance matrix and treated this as a phylogenetic tree to evaluate whether there was a signal for abundance in the defense data. There was not (Peru: $K = 0.12$, $P = 0.85$; Panama: $K = 0.59$, $P = 0.62$), and we therefore shuffled species labels in the defense distance matrix to generate null communities for defense trait structure analyses.

We evaluated whether the distribution of NRI and NTI values for communities were significantly different from zero by using t tests following Kembel and Hubbell (17). All phylogenetic and defense trait structure analyses were conducted by using functions in the Picante and APE packages in R (http://picante.r-forge.r-project.org).

We also conducted defense community structure analyses by using the first two axes from the PCA above to represent developmental and ant defense trait variation. Specifically, we averaged the chemical distance matrices with a distance matrix derived from the Euclidean distance between species along the first two principal component axes. This necessarily resulted in a loss of sample size, with regard to species, for Peru because many species were lacking expansion and chlorophyll data. This analysis gave results in the same direction as the above analyses (Panama: $\tilde{\text{NRI}} = 0.48$, $t = 8.74$, $P < 0.00001$; $\tilde{\text{NTI}} = 0.59$, $t = 10.53$, $P < 0.00001$; Peru: $\tilde{\text{NRI}} = 0.08$, $t = 0.34$, $P = 0.370$; $\tilde{\text{NTI}} = 0.24$, $t = 1.36$, $P = 0.092$).

To determine whether other traits, not related to herbivore defense, showed a similar pattern of community structure, we obtained data for each species on the presence of wings on the leaf rachis and the number of leaflets per leaf (Table S3). We created a distance matrix for calculation of NRI and NTI values by averaging distance matrices for the first two axes from a PCA of these characters.

1. Dexter KG (2008) The effects of dispersal on macroecological patterns. PhD Thesis (Duke University, Durham, NC).
2. Shaw J, Lickey EB, Schilling EE, Small RL (2007) Comparison of whole chloroplast genome sequences to choose noncoding regions for phylogenetic studies in angiosperms: The tortoise and the hare III. *Am J Bot* 94:275–288.
3. Hollingsworth ML, et al. (2009) Selecting barcoding loci for plants: Evaluation of seven candidate loci with species-level sampling in three divergent groups of land plants. *Mol Ecol Res* 9:439–457.
4. Huelsenbeck JP, Ronquist F (2001) MRBAYES: Bayesian inference of phylogenetic trees. *Bioinformatics* 17:754–755.
5. Posada D, Crandall KA (1998) MODELTEST: Testing the model of DNA substitution. *Bioinformatics* 14:817–818.

6. Sanderson MJ (1997) A nonparametric approach to estimating divergence times in the absence of rate constancy. *Mol Biol Evol* 14:1218–1231.
7. Paradis E, Claude J, Strimmer K (2004) APE: Analyses of phylogenetics and evolution in R language. *Bioinformatics* 20:289–290.
8. Garland T, Harvey PH, Ives AR (1992) Procedures for the analysis of comparative data using phylogenetically independent contrasts. *Syst Biol* 41:18–32.
9. Legendre P, Legendre L (1998) *Numerical Ecology* (Elsevier, Amsterdam), 2nd Ed.
10. Everitt BS, Landau S, Leese M (2001) *Cluster Analysis* (Taylor & Francis, Florence, KY), 4th Ed.
11. Suzuki R, Shimodaira H (2006) Pvclust: An R package for assessing the uncertainty in hierarchical clustering. *Bioinformatics* 22:1540–1542.
12. Blomberg SP, Garland T, Jr, Ives AR (2003) Testing for phylogenetic signal in comparative data: Behavioral traits are more labile. *Evolution (Lawrence, Kans)* 57:717–745.
13. Kursar TA, Coley PD (2003) Convergence in defense syndromes of young leaves in tropical rainforests. *Biochem Syst Ecol* 21:929–949.
14. Maddison WP, Maddison DR (2007) *Mesquite: A Modular System for Evolutionary Analysis* (Mesquite Software, Austin, TX).
15. Maddison D, Maddison W (2005) *MacClade, Version 4.08* (Sinauer, Sunderland, MA).
16. Webb CO (2000) Exploring the phylogenetic structure of ecological communities: An example for rain forest trees. *Am Nat* 156:145–155.
17. Kembel SW, Hubbell SP (2006) The phylogenetic structure of a Neotropical forest tree community. *Ecology* 87:S86–S99.
18. Hardy OJ (2008) Testing the spatial phylogenetic structure of local communities: Statistical performances of different null models and test statistics on a locally neutral community. *J Ecol* 96:914–926.
19. Xie D-Y, Dixon RA (2005) Proanthocyanidin biosynthesis: Still more questions than answers? *Phytochemistry* 66:2127–2144.

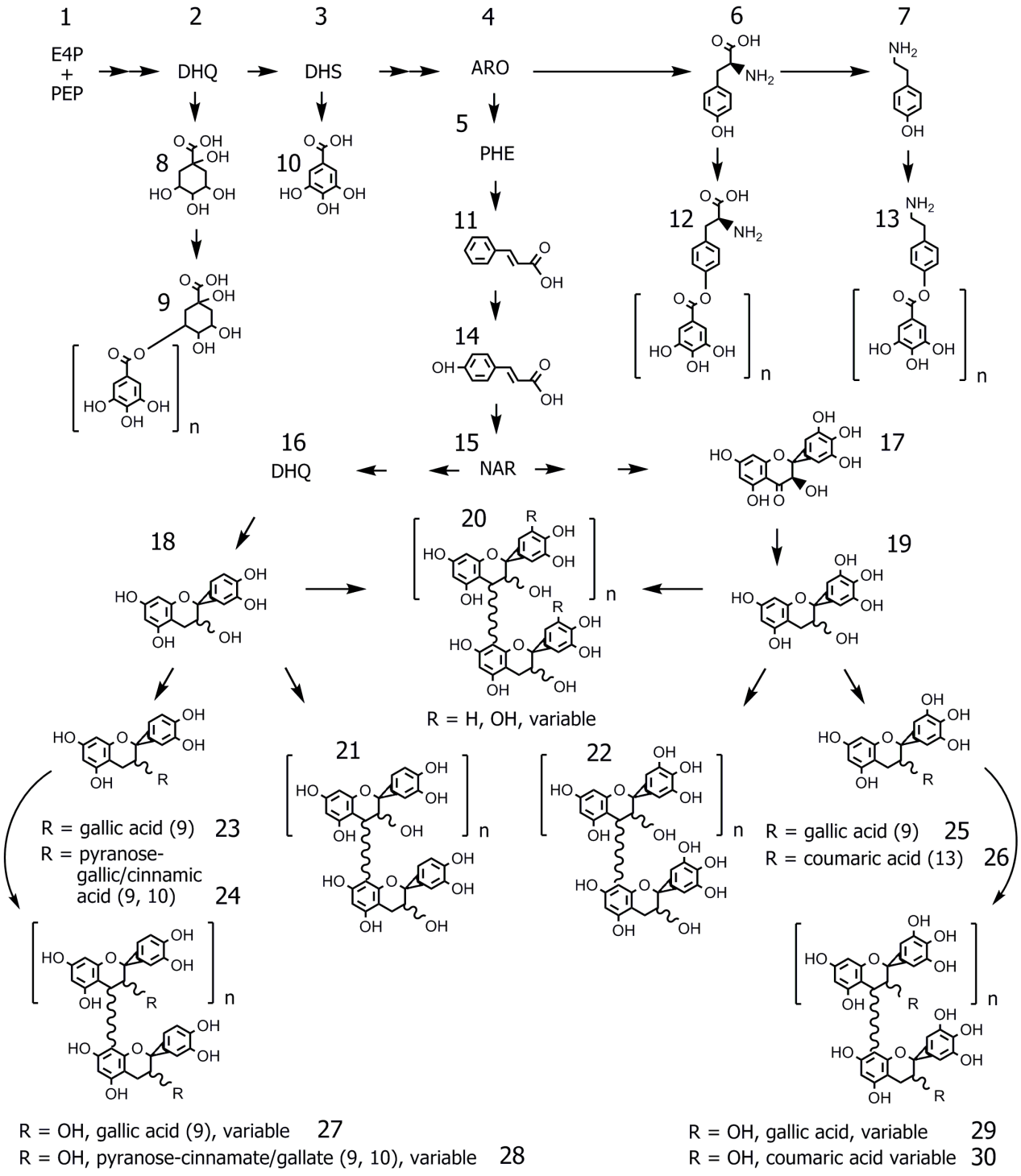

Fig. S1. Important shikimic acid/phenylpropanoid/flavonoid pathway intermediates and branch points in *Inga*. Only a subset of the biosynthetic steps are shown. The acronyms refer to biosynthetic precursors and biosynthetic intermediates. The precursors include **1**, erythrose-4-phosphate + phosphoenolpyruvate; **2**, dehydroquinic acid; **3**, dehydroshikimic acid; **4**, L-arogenate, and **5**, phenylalanine. The biosynthetic intermediates are **15**, naringenin and **16**, dihydroquercetin. The structures of the intermediate adducts, the compounds that do not accumulate to a high level in vivo as monomers but that are components of important defense metabolites, include: **7**, tyramine; **8**, quinic acid; **10**, gallic acid; **11**, cinnamic acid, and **14**, coumaric acid. The 18 end-products, the major defense metabolites that accumulate to a high level in vivo, are: **6**, tyrosine; **9**, quinic acid gallate; **12**, tyrosine gallate; **13**, tyramine gallate; **17**, dihydromyricetin; **18**, catechin/epicatechin (*c*/e); **19**, gallocatechin/galloepicatechin (gc/ge); **20**, mixed *c*/e-gc/ge polymer; **21**, *c*/e polymer; **22**, gc/ge polymer; **23**, 3-*O*-galloyl *c*/e; **24**, 3-*O*-pyrano-galloyl/cinnamoyl *c*/e; **25**, 3-*O*-galloyl gc/ge; **26**, 3-*O*-coumaroyl gc/ge; **27** and **28**, *c*/e polymer variably substituted at the 3-*O*- position; **29** and **30**. gc/ge polymer variably substituted at the 3-*O*- position. Six of the 18 listed end-products, **18**, **19**, and **23**-**26**, are also the monomeric building blocks of the indicated polymers. The other 12 end-products correspond to the 12 classes of phenolics referred to in *Results*. After Xie and Dixon (19).

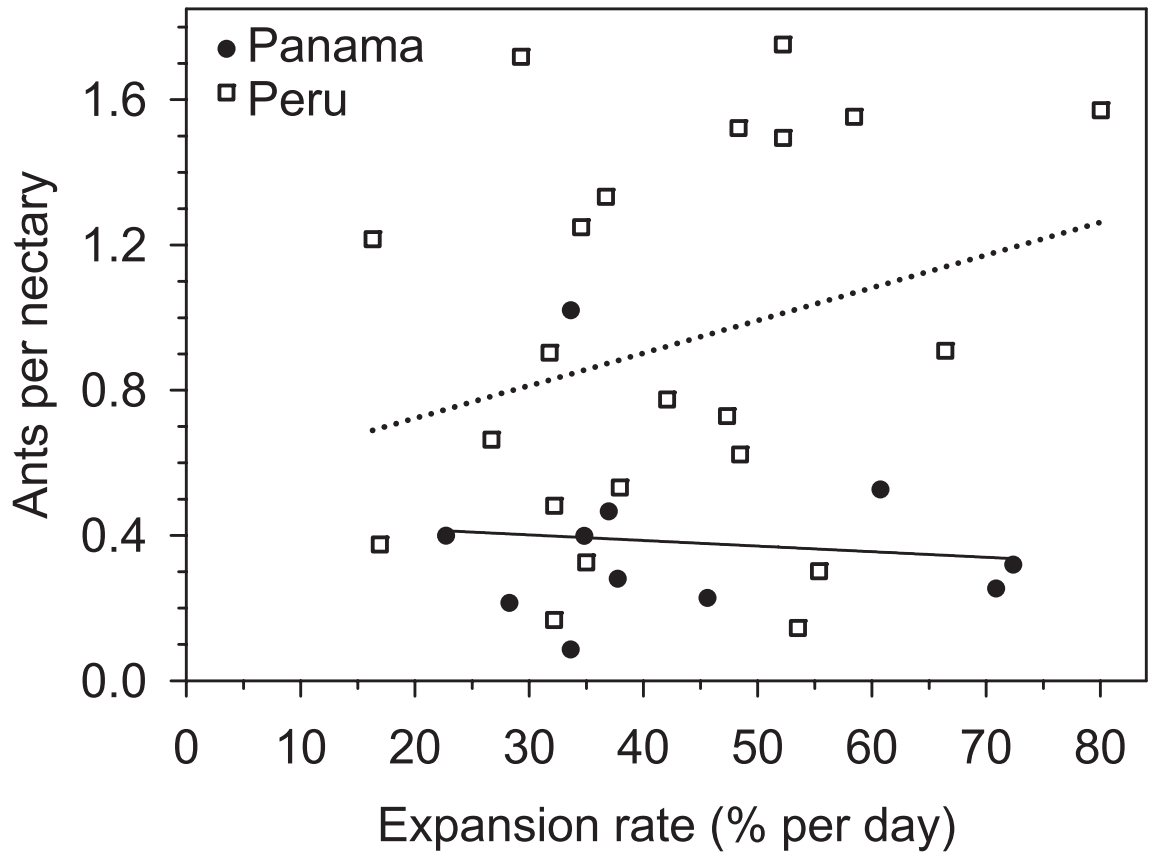

Fig. S2. The rate of expansion of young leaves expressed as the percentage increase in area per day (% per day) versus the number of ants visiting extrafloral nectaries on young leaves of *Inga* species. There was no significant relationship for either Panama (solid line, $r^2 = 0.11$, $P = 0.75$, $n = 11$) or Peru (dotted line, $r^2 = 0.069$, $P = 0.24$, $n = 22$).

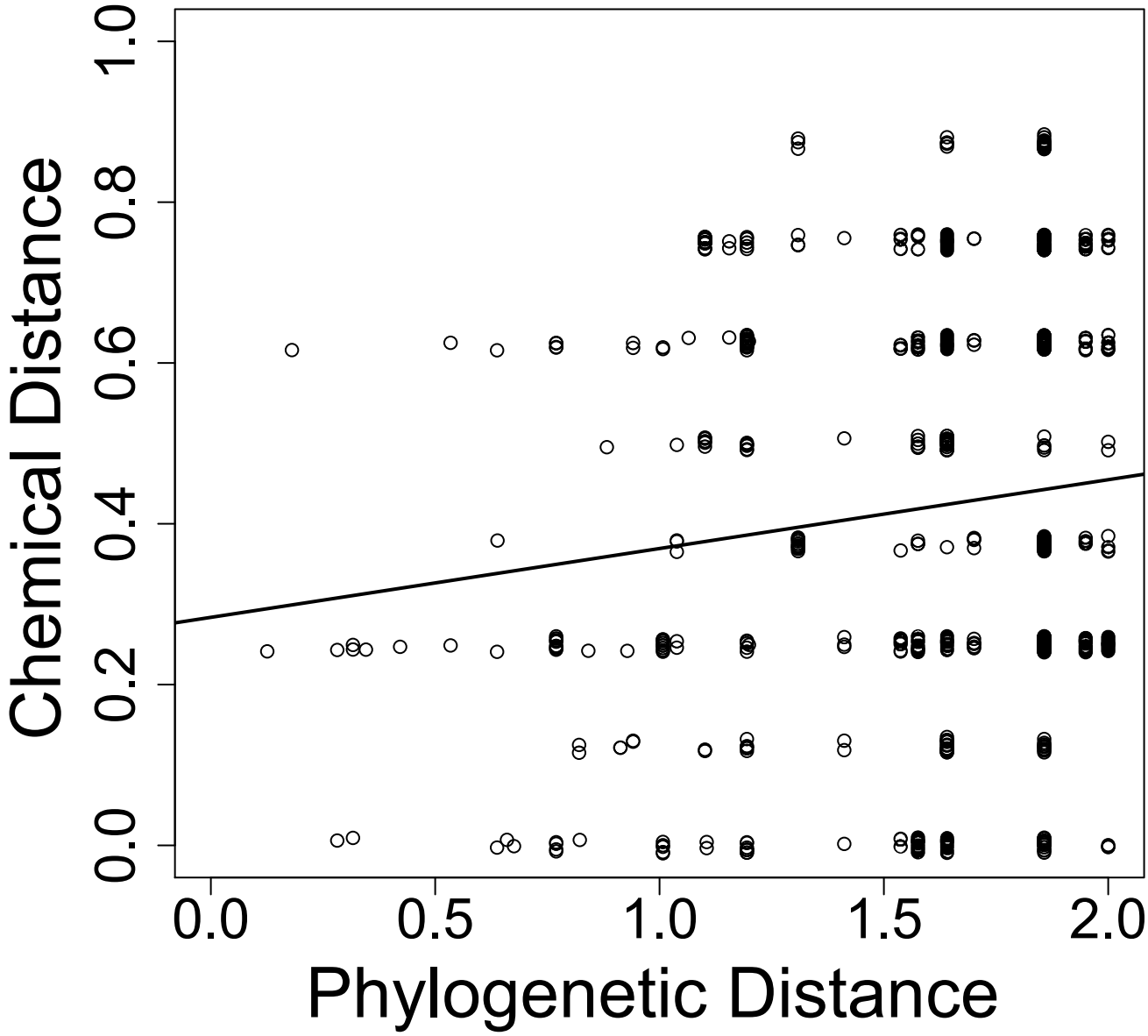

Fig. S3. Average chemical distance (weighting phenolics and saponins equally) between species by phylogenetic distance between species for one randomly selected Bayesian tree. The line represents the best-fit linear regression ($y = 0.28 + 0.086x$), while significance and fit of the relationship was evaluated by using a Mantel test (for this tree: $r = 0.12$, $P = 0.031$).

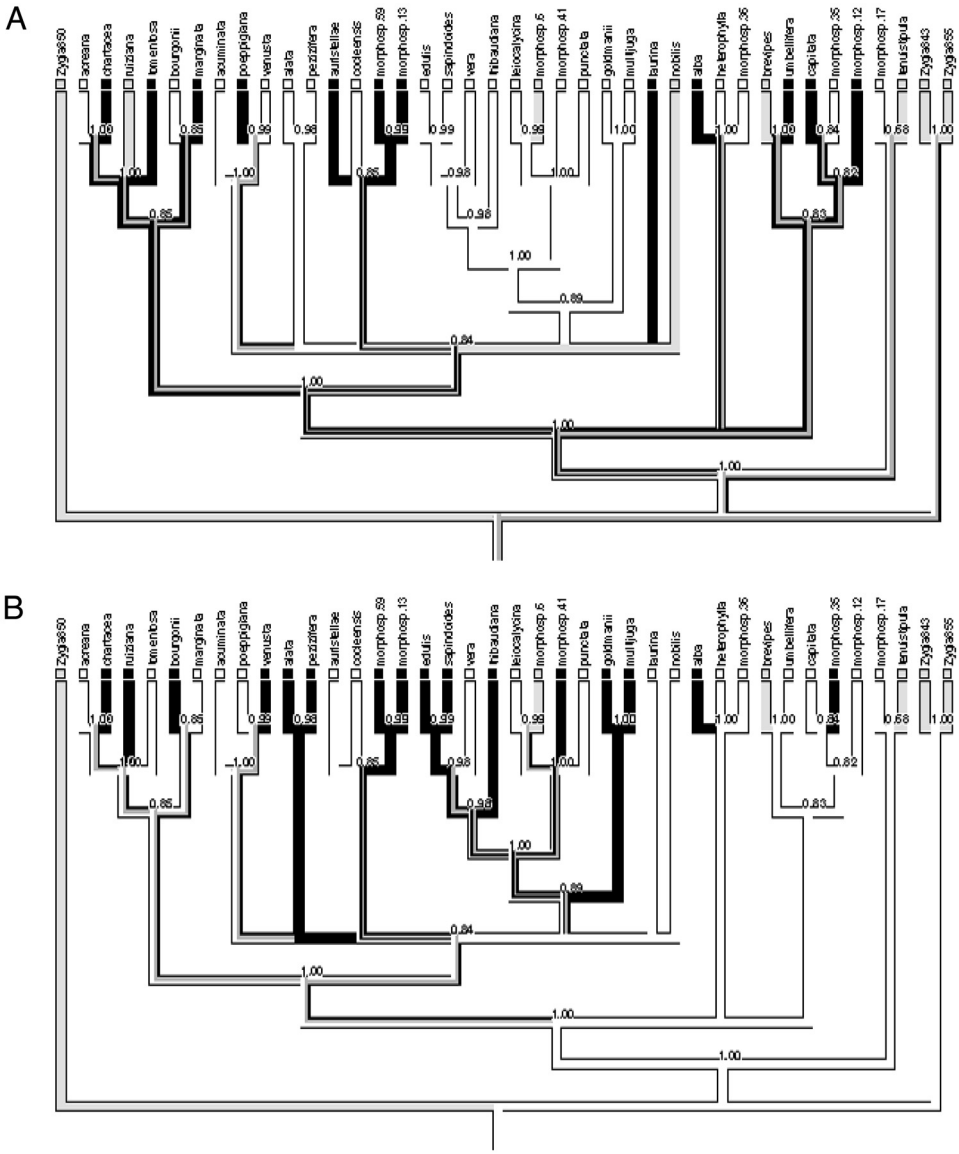

Fig. S4. Developmental and ant defense mapped onto *Inga* phylogeny. (*A*) Binary character of defense (white) and escape (black) optimized by using parsimony onto 50% majority rule Bayesian consensus tree (gray shading indicates equivocal state). Numbers adjacent to nodes are posterior probability values. To account for topological uncertainty, ancestral state reconstruction was summarized for >100 Bayesian trees sampled at stationarity, and along each branch the thickness of the line representing each state is in proportion to the number of trees in which that state is reconstructed. Low phylogenetic signal is indicated by 8–11 observed parsimony steps, which is well within the frequency distribution of the number of steps when states are randomized across terminal taxa (''reshuffle character'' option in Mesquite 2.01) (14). Furthermore, the 8–11 observed transformations lie within the frequency distribution of transformations when mapped onto 1,000 random trees generated by MacClade 4.08 (15). (*B*) Binary character of low (white) and high (black) ant visitation (gray shading indicates equivocal state) optimized using parsimony onto 50% majority rule Bayesian consensus tree. Numbers adjacent to nodes are posterior probability values. To account for topological uncertainty, ancestral state reconstruction was summarized for >100 Bayesian trees sampled at stationarity, and along each branch the thickness of the line representing each state is in proportion to the number of trees in which that state is reconstructed. Low phylogenetic signal is indicated by 10–13 observed parsimony steps, which is well within the frequency distribution of transformations when randomized across terminal taxa (reshuffle character option in Mesquite 2.01) (14). Furthermore, the 10–13 observed transformations lie within the frequency distribution of transformations when mapped onto 1,000 random trees generated by MacClade 4.08 (15).

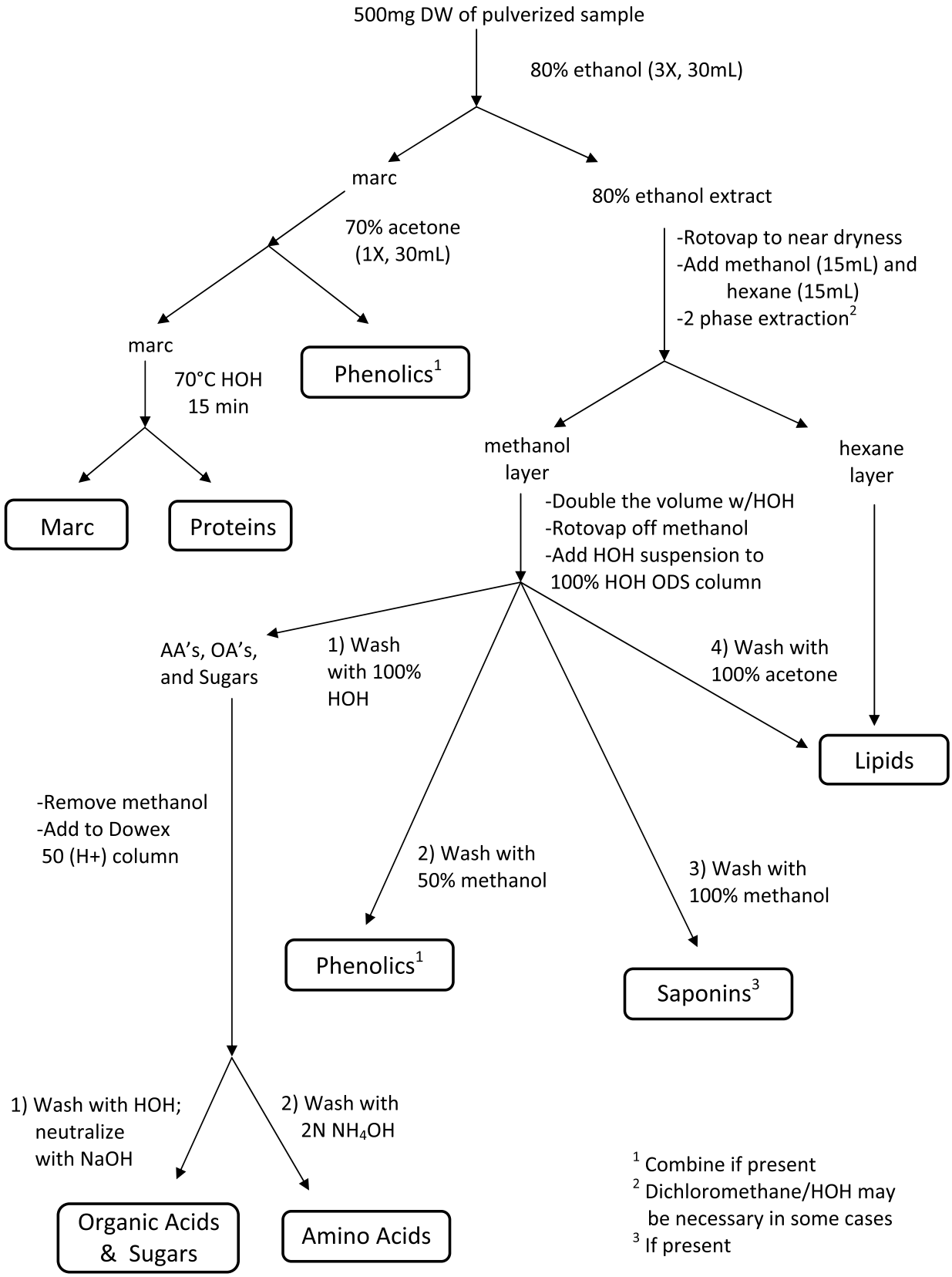

Fig. S5. The protocol used to resolve *Inga* young leaf extracts into chemically distinct fractions. The term "marc" refers to the insoluble cell walls. ODS refers to liquid chromatography on an octadecyl silane (or reversed-phase silica) column. AA, amino acids; OA, organic acids.

Table S1. Distributions of *Inga* chemotypes

Chemotype	No. of species
Phenolic/saponin	
Gallocatechin/epigallocatechin gallate	11
Saponin	5
Catechin/epicatechin	4
Gallocatechin/epigallocatechin gallate + saponin	4
Quinic acid-gallate	2
Catechin/epicatechin-methyl pyranose gallate	2
Catechin/epicatechin + saponin	2
Tyrosine gallate	2
Catechin-epicatechin gallate	1
Catechin-epicatechin-pyranose-phenolic acid + tyrosine	1
Flavone	1
Gallocatechin/epigallocatechin-gallate-coumarate + saponin	1
Tyramine gallate + quinic acid gallate	1
Amino acid	
Monohydroxypipecolic acid #2 + dihydroxypipecolic acid #2	4
5-Amino-4-hydroxypentanoic acid + *N*-methyl-hydroxyproline	1
Monohydroxypipecolic acid #3	1
Monohydroxypipecolic acid #1	1
Dihydroxypipecolic acid #4	1
Monohydroxypipecolic acid #3 + dihydroxypipecolic acid #1 + 2	1
Monohydroxypipecolic acid #3 + djenkolic acid	1
Tyrosine	1

Each chemotype is a distinct combination of metabolites. Shown are the major phenolic/saponin chemotypes for all 37 study species (Peru and Panama) and the major amino acid chemotypes for 11 study species from Panama.

Table S2. Gallocatechin/galloepicatechin gallate structures (cf. Fig. S1) inferred from MS analysis of *Cojoba arboreab* phenolic extracts and shared among 11 of the 37 *Inga* study species

Nominal mass	Gallocatechin-galloepicatechin no.	Gallate no.
458	1	1
762	2	1
914	2	2
1066	3	1
1218	3	2
1370	3	3
1370	4	1
1522	4	2
1522	5	0
1674	4	3
1674	5	1

The nominal mass refers to the actual mass, in atomic mass units, of the polymer rounded to the nearest integer. Each unit of the polymer contains either one gallocatechin or one galloepicatechin. These are identical in molecular formula and differ in stereochemistry. Therefore, the degree of polymerization is noted as gallocatechin-galloepicatechin no. The number of gallate esters is noted as gallate no. The minimum esterification with gallate is zero on the entire polymer (e.g. nominal mass 1,522, a tetramer with no gallate). The maximum esterification is one for every gallocatechin/galloepicatechin unit of the polymer (e.g. nominal mass 1,370, a trimer with three gallates). Because the table is ordered by nominal mass and because of the variation in the number of gallates per polymer, gallocatechin-galloepicatechin no. is not in numerical order. Polymers at masses in excess of the highest shown, 1,674, exist and are minor components. In the species of *Inga* characterized to date, the gallocatechin/galloepicatechins and gallic acids polymerize such that a dimer could, in principle, have eight or more forms of identical mass. Although not indicated here, we observe a subset of the possible forms of dimers, trimers, tetramers, and pentamers. These forms are distinguished as having identical masses but often distinct chromatographic behavior; they have not been fully characterized.

Table S3. Average values for the leaf traits of *Inga* species from Panama and Peru, including chlorophyll content of young leaves, rates of young-leaf expansion, and the number of ants censused at extrafloral nectaries (mean, SE, and *n*)

Inga species	Chlorophyll ($mg \cdot m^{-2}$)	Chlorophyll SE	Chlorophyll # plants	Expansion ($\% \ d^{-1}$)	Expansion SE	Expansion # plants	Escape or defense	# Ants per extrafloral nectary	Ants SE	Ants # plants	Ants-normalized	Wings on the rachis	# Leaflets per leaf
Panama													
acuminata	111	17	11	33.6	2.1	12	D	0.1	0.0	282	L	Y	12
cocleensis	89	10	11	37.7	1.8	18	D	0.3	0.0	455	L	N	14
laurina	65	5	9	70.9	2.5	11	E	0.3	0.0	139	L	N	4
goldmanii	85	5	9	33.6	0.7	18	D	1.0	0.2	219	H	Y	8
marginata	36	5	10	72.4	5.9	21	E	0.3	0.0	253	L	Y	4
multijuga	128	6	8	22.7	1.4	12	D	0.4	0.1	46	H	N	16
pezizifera	103	10	11	34.8	0.7	17	D	0.4	0.0	314	H	N	8
nobilis	49	6	13	60.7	2.8	18	E	0.5	0.2	182	H	N	8
ruiziana								0.8	0.3	5	H	N	10
sapindoides	78	7	11	36.9	1.6	15	D	0.5	0.0	275	H	Y	6
umbellifera	28	3	15	45.6	3.2	16	E	0.2	0.0	233	L	Y	6
vera	119	9	7	28.3	1.1	22	D	0.2	0.1	28	L	Y	10
Peru													
acreana	95	4	9	32.2	1.5	22	D	0.2	0.1	19	L	Y	6
alata	122	6	8	29.3	1.0	9	D	1.7	0.7	11	H	Y	12
alba	63	6	7	80.0	2.9	18	E	1.6	0.2	91	H	Y	8
auristellae	20	3	11	48.5	1.9	19	E	0.6	0.1	62	L	Y	6
bourgonii	103	7	8	52.2	2.5	7	D	1.8	0.6	21	H	Y	6
brevipes	46	2	7	58.4	2.0	8	E	1.6	0.4	12	H	Y	4
capitata	75	4	9	42.1	2.9	7	E	0.8	0.2	13	L	N	4
chartacea	63	4	8	36.7	2.5	9	E	1.3	0.3	36	H	Y	6
edulis	71	6	8	52.2	3.1	19	D	1.5	0.2	127	H	Y	8
heterophylla	61	4	8	53.5	3.1	23	D	0.1	0.0	66	L	N	8
laurina	50	4	4	55.4	2.4	2	E	0.3	0.2	6	L	N	4
leiocalycina	112	6	9	26.7	0.6	12	D	0.7	0.1	51	L	N	4
marginata							E	0.6	0.5	4	L	Y	4
morphosp.12							E					N	4
morphosp.13	66	5	10	66.4	2.2	13	E	0.9	0.1	45	H	N	6
morphosp.17	110	8	9	35.0	1.8	10	D	0.3	0.2	23	L	N	8
morphosp.35	90	4	7	16.3	1.6	6	D	1.2	0.4	48	H	N	4
morphosp.36	74	8	3				D	0.1	0.0	8	L	N	12
morphosp.41	107	7	7	31.8	1.0	6	D	0.9	0.4	8	H	N	8
morphosp.59	70	2	10	48.3	3.2	10	E	1.5	0.5	26	H	N	4
morphosp.6								0.4	0.3	6	L	N	4
nobilis								0.6	0.5	5	L	N	14
poeppigiana	56	6	12	32.2	2.0	14	E	0.5	0.1	42	L	Y	6
punctata				19.7	0.4	2	D	0.7	0.3	4	L	N	4
ruiziana	79	4	5					0.4	0.5	3	L	N	8
tenuistipula	151	26	3	16.9	0.3	2	D	0.4	0.2	8	L	N	6
thibaudiana	120	14	8	34.5	1.9	15	D	1.2	0.2	124	H	N	12
tomentosa	84	6	7	47.3	1.9	26	E	0.7	0.2	39	L	Y	6
umbellifera	40	5	8	37.9	2.6	6	E	0.5	0.1	27	L	Y	4
venusta	156	19	7	21.4	3.9	6	D	9.5	5.1	23	H	Y	6

Developmental strategies of escape or defense were assigned based on chlorophyll and expansion (see Fig. 2). Because ant visitation was different between sites, we characterized the numbers of ants at nectaries as high (H) if they were above the site average or low (L) if they were below the site average. The presence or absence of wings on the rachis and the number of leaflets per leaf were determined for saplings in the field.

Table S4. Collection details and GenBank accession numbers of material used for phylogenetic study

Taxon	Voucher details	Country	Locality	Herbarium	GenBank accession nos.					
					trnL-trnF	*trnD-trnT*	*trnH-psbA*	*rps16*	*rpoC1*	*ndhF-rpl32*
Zygia 843	Kyle Dexter 843	Peru	Madre de Dios	Duke	GQ118709	FJ974145	GQ118858	GQ118826	GQ118787	GQ118748
Zygia 850	Kyle Dexter 850	Peru	Madre de Dios	Duke	GQ118710	FJ974151	GQ118859	GQ118827	GQ118788	GQ118749
Zygia 855	Kyle Dexter 855	Peru	Madreselva, Loreto	Duke	GQ118711	GQ871278	GQ118860	GQ118828	GQ118789	GQ118750
Inga acreana Harms	Kyle Dexter 390	Peru	Madre de Dios, Los Amigos	Duke	GQ118712	FJ974164	GQ118861	GQ118829	GQ118790	GQ118751
Inga acuminata Benth.	Thomas Kursar & Phyllis Coley 1266	Panama	Barro Colorado Island	K, STRI	GQ118713	GQ871263	GQ118862	GQ118830	GQ118791	GQ118752
Inga alata Benoist	Kyle Dexter 402	Peru	Madre de Dios, Los Amigos	K	GQ118714	FJ974180	GQ118863	GQ118831	GQ118792	GQ118753
Inga alba (Sw.)Willd.	Kyle Dexter 494	Peru	Madre de Dios, Los Amigos	K	GQ118715	FJ974241	GQ118864	GQ118832	GQ118793	GQ118754
Inga auristellae Harms	Kyle Dexter 10	Peru	Madre de Dios, Los Amigos	K	GQ118716	FJ974279	GQ118865	GQ118833	GQ118794	GQ118755
Inga bourgonii (Aubl.)DC.	Kyle Dexter 404	Peru	Madre de Dios, Los Amigos	K	GQ118717	FJ974351	GQ118866	GQ118834	GQ118795	GQ118756
Inga brevipes Benth.	Kyle Dexter 202	Peru	Madre de Dios, Los Amigos	K	GQ118718	FJ974409	GQ118867	-	GQ118796	GQ118757
Inga capitata Desv.	Thomas Kursar & Phyllis Coley 1568	Peru	Madre de Dios, Los Amigos	MOL	GQ118719	GQ871264	-	GQ118835	GQ118797	GQ118758
Inga chartacea Poepp. & Endl.	Kyle Dexter 358	Peru	Madre de Dios, Los Amigos	K	GQ118720	FJ974449	GQ118868	GQ118836	GQ118798	GQ118759
Inga cocleensis Pittier	Thomas Kursar & Phyllis Coley 1273	Panama	Barro Colorado Island	K, STRI	GQ118721	GQ871265	GQ118869	GQ118837	GQ118799	GQ118760
Inga edulis Mart.	Kyle Dexter 386	Peru	Madre de Dios, Los Amigos	K	GQ118722	FJ974509	GQ118870	GQ118838	GQ118800	GQ118761
Inga goldmanii Pittier	Thomas Kursar & Phyllis Coley 1271	Panama	Barro Colorado Island	K, STRI	GQ118723	GQ871266	GQ118871	GQ118839	GQ118801	GQ118762
Inga heterophylla Willd.	Thomas Kursar & Phyllis Coley 1528	Peru	Madre de Dios, Los Amigos	MOL	GQ118724	GQ871267	-	-	GQ118802	-
Inga morphosp.36	Thomas Kursar & Phyllis Coley 1545	Peru	Madre de Dios, Los Amigos	MOL	GQ118725	GQ871268	-	-	GQ118803	GQ118763
Inga morphosp.59	Thomas Kursar & Phyllis Coley 1635	Peru	Madre de Dios, Los Amigos	MOL	GQ118726	GQ871269	GQ118872	-	GQ118804	GQ118764
Inga leiocalycina Benth.	Thomas Kursar & Phyllis Coley 1593	Peru	Madre de Dios, Los Amigos	MOL	GQ118727	GQ871270	-	-	GQ118805	GQ118765
Inga marginata Willd.	Kyle Dexter 463	Peru	Madre de Dios, Los Amigos	K	GQ118728	FJ974628	GQ118873	GQ118840	GQ118806	GQ118766
Inga morphosp.13	Kyle Dexter 29	Peru	Madre de Dios, Los Amigos	K	GQ118729	FJ974988	GQ118874	GQ118841	GQ118807	GQ118767
Inga morphosp.41	Kyle Dexter 37	Peru	Madre de Dios, Los Amigos	K	GQ118730	FJ975003	GQ118875	GQ118842	GQ118808	GQ118768
Inga morphosp.17	Kyle Dexter 53	Peru	Madre de Dios, Los Amigos	K	GQ118731	FJ975011	GQ118876	GQ118843	GQ118809	GQ118769
Inga morphosp.12	Kyle Dexter 349	Peru	Madre de Dios, Los Amigos	K	-	FJ974438	-	-	GQ118810	GQ118770
Inga laurina (Sw.)Willd.	Kyle Dexter 526	Peru	Madre de Dios, Los Amigos	Duke	GQ118732	FJ975039	GQ118877	GQ118844	GQ118811	GQ118771
Inga multijuga Benth.	Thomas Kursar & Phyllis Coley 1274	Panama	Barro Colorado Island	K, STRI	GQ118733	GQ871271	GQ118878	GQ118845	GQ118812	GQ118772
Inga nobilis Willd.	Kyle Dexter 163	Peru	Madre de Dios, Los Amigos	K	GQ118734	FJ974673	GQ118879	GQ118846	GQ118813	GQ118773
Inga pezizifera Benth.	Thomas Kursar & Phyllis Coley 1001	Panama	Barro Colorado Island	K, STRI	GQ118735	GQ871272	GQ118880	GQ118847	GQ118814	GQ118774
Inga poeppigiana Benth.	Kyle Dexter 85	Peru	Madre de Dios, Los Amigos	K	GQ118736	FJ974683	GQ118881	GQ118848	-	GQ118775
Inga punctata Willd.	Kyle Dexter 475	Peru	Madre de Dios, Los Amigos	K	GQ118737	FJ974713	GQ118882	GQ118849	GQ118815	GQ118776
Inga ruiziana G.Don	Thomas Kursar & Phyllis Coley 1256	Panama	Barro Colorado Island	K, STRI	GQ118738	GQ871273	GQ118883	GQ118850	GQ118816	GQ118777
Inga sapindoides Willd.	Thomas Kursar & Phyllis Coley 1264	Panama	Barro Colorado Island	K, STRI	GQ118739	GQ871274	GQ118884	GQ118851	GQ118817	GQ118778
Inga morphosp.6	Thomas Kursar & Phyllis Coley 1561	Peru	Madre de Dios, Los Amigos	MOL	GQ118740	GQ871275	-	-	GQ118818	GQ118779
Inga morphosp.35	Thomas Kursar & Phyllis Coley 1560	Peru	Madre de Dios, Los Amigos	MOL	GQ118741	GQ892055	-	-	GQ118819	GQ118780
Inga tenuistipula Ducke	Kyle Dexter 110	Peru	Madre de Dios, Los Amigos	K	GQ118742	FJ974870	GQ118885	GQ118852	GQ118820	GQ118781
Inga thibaudiana DC.	Kyle Dexter 340	Peru	Madre de Dios, Los Amigos	K	GQ118743	FJ974883	GQ118886	GQ118853	GQ118821	GQ118782
Inga tomentosa Benth.	Kyle Dexter 102	Peru	Madre de Dios, Los Amigos	K	GQ118744	FJ974910	GQ118887	GQ118854	GQ118822	GQ118783
Inga umbellifera (Vahl)Steud.	Thomas Kursar & Phyllis Coley 1318 (collected by S Ring and B Wolfe)	Panama	Barro Colorado Island	K, STRI	GQ118745	GQ871276	GQ118888	GQ118855	GQ118823	GQ118784

Taxon	Voucher details	Country	Locality	Herbarium	GenBank accession nos.					
					trnL-trnF	*trnD-trnT*	*trnH-psbA*	*rps16*	*rpoC1*	*ndhF-rpl32*
Inga venusta Standl.	Kyle Dexter 78	Peru	Madre de Dios, Los Amigos	K	GQ118746	FJ974975	GQ118889	GQ118856	GQ118824	GQ118785
Inga vera Willd.	Thomas Kursar & Phyllis Coley 1308 (collected by D Dvorett and S Ring)	Panama	Barro Colorado Island	K, STRI	GQ118747	GQ871277	GQ118890	GQ118857	GQ118825	GQ118786

Duke, Duke University, Durham, NC; K, Royal Botanic Gardens, Kew, United Kingdom; STRI, Smithsonian Tropical Research Institute, Balboa, Panama; MOL, Universidad Nacional Agraria, La Molina, Lima, Peru. Dash indicates no sequence was obtained.